Development of Intraoperative Beta Probes Based on Silicon Photomultipliers

N. Hudin, L. Pinot, Y. Charon, N. Dinu, T. Ait Imando, B. Janvier, V. Puill, D. Benoit, M.-A. Duval, L. Menard

PROCEEDINGS OF SCIENCE

Design and simulation of an intraoperative Positron Probe based on Silicon Photomultipliers

N. Hudin
Laboratoire Imagerie et Modélisation en Neurobiologie et Cancérologie, IN2P3-CNRS
91406 Orsay, France.
E-mail: hudin@imnc.in2p3.fr

L. Pinot[a], Y. Charon[a], N. Dinu[b], T. Ait Imando[b], B. Janvier[a], V. Puill[b], D. Benoit[a], M-A Duval[a], L. Ménard[a]
[a] *Laboratoire Imagerie et Modélisation en Neurobiologie et Cancérologie, IN2P3-CNRS*
91406 Orsay, France.
[b] *Laboratoire de l'Accélérateur Linéaire, IN2P3-CNRS*
91898 Orsay, France.

Intraoperative positron probes present intrinsic advantages over gamma detection to perform tumor localization and post-operative control of the surgical cavity during surgery. In that context, Silicon Photomultiplier (SiPM) introduced a breakthrough for the development of miniaturized imaging devices. We report here the results of a simulation study aiming to optimize the design of a positron imaging probe based on plastic scintillators coupled to SiPM photosensors. Two different γ ray background rejection schemes were investigated. The first one consists of a stack of two SiPM arrays each coupled to a continuous plastic scintillator. The second configuration implements two layers of plastic scintillator separated by a light guide and read-out by a single SiPM array. Events originating from the top and the bottom layers are discriminated from the analysis of the light distribution on the photosensor. We first showed that a subtraction method can perform very good rejection up to 98% of the background gamma noise with a weak sensitivity to its distribution when the gap between the two scintillators is smaller than 4 mm. We also demonstrated that both configurations of the positron imaging probe can offer sub-millimetric resolutions and very small bias.

International Workshop on New Photon-detectors,
LAL Orsay, France
June 13-15, 2012

1. Introduction

Quality of surgical excision of a tumor is determined by the ability to remove the biggest part of malignant cells while sparing surrounding normal tissues. In that context, precise delineation of the tumor boundaries is a crucial information to realize the most efficient surgery. Recent studies have shown the feasibility and the clinical potential of intraoperative localization to localize in real time radiolabeled tumors [1,2]. Alongside medium and high-energy gamma counting or imaging systems, in situ detection of short-range particles, such as positrons, exhibits intrinsic advantages to increase the tumor signal-to-noise ratio by avoiding count rate contamination from distal non-specific accumulation area of radiotracers [3,4]. The short range of beta particles can also be used to design light hand-held detection systems with overall sensitivity between one and three orders of magnitude higher than that of gamma detection probes, because no collimation is needed. Among the alternative photosensors that have been developed and implemented during the last ten years, Silicon Photomultipliers (SiPM) have the potential to fulfill most of the needs to achieve efficient intraoperative positron detection (high signal-to-noise ratio, compactness, low weight, simplicity of implementation and versatility) and to notably impact the performances of future intraoperative devices.

In that context, we are currently developing a small field of view (~5cm^2) positron imaging probe based on plastic scintillators and SiPM photosensors to perform tumor localization and post-operative control of the surgical cavity. In order to achieve optimal performances, Monte Carlo simulations were conducted to investigate the impact of the detection head design, including different background rejection schemes, on the spatial performances and gamma ray rejection efficiency of the positron imaging probe.

2. Materials and Methods

2.1 Design of the intraoperative positron imaging probe

The key features when trying to localize small amount of tumor tissue labeled with positron emitters are sensitivity and γ ray rejection efficiency. Different rejection methods can be considered to eliminate the background noise coming from the high flux of 511keV annihilation γ rays [5]. To achieve good rejection capability while maintaining the compactness of the probe, we choose to implement real-time subtraction schemes based on a stack of two thin scintillators. The amount of gamma photons contamination is estimated by the rear detector shielded to beta particles by the front detector. We obtain a gamma-free positron image by subtracting this contamination from the count rate distribution measured with the front detector after applying a suitable weighting factor. We investigated two different background subtraction schemes based on one or two small size photodetection SiPM-modules with four 16-channel monolithic SiPM arrays composed of 3x3 mm^2 elements with 50x50µm microcells (Hamamatsu, S11828-3344M) (fig.1). The first one is based on the stack of two SiPM arrays each coupled to a continuous plastic scintillator (BC 400, St Gobain) through a PMMA light guide. The second configuration implements two layers of plastic scintillator separated by a light guide. This assembly is mounted onto a single SiPM array. Events originating from the top and the bottom layers are discriminated from the analysis of the light distribution on the photosensor. We simulated two types of plastic scintillators for the bottom layer: a continuous scintillator and a pixelated array. The thickness of all scintillators was set to 0.5 mm. This value was shown to provide the optimal performances in terms of electron energy deposition from ^{18}F sources and minimal contamination from background γ rays [6].

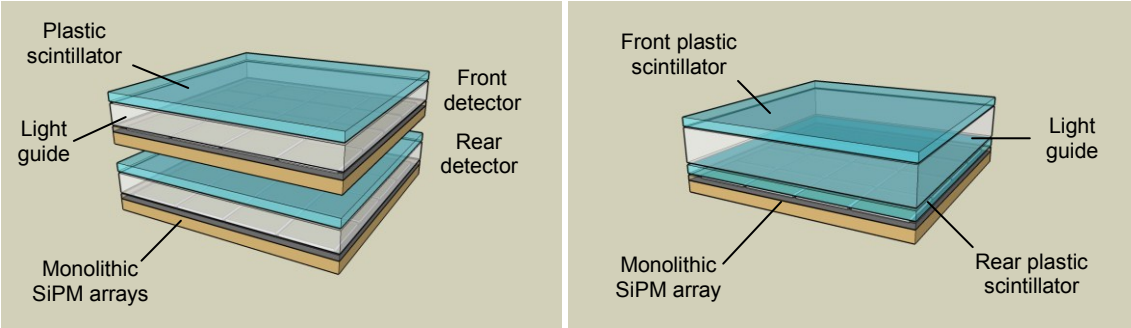

Fig.1. Designs of the positron imaging probe. The first configuration is based on the stack of two SiPM arrays each coupled to a thin continuous plastic scintillator (left). The second configuration consists of two plastic scintillators separated by a light guide and coupled to a single SiPM array.

2.2 Simulation study

Simulations were performed using the GATE Monte-Carlo simulation platform. The simulation study was divided into two parts: the evaluation of the gamma ray rejection efficiency of the subtraction method as a function of the distance between the two scintillators and the imaging capabilities of the positron probe for the two background rejection configurations. To speed up the simulation, only one quarter of the detection field of view (13.6x13.6 mm^2) was modelled.

2.2.1 Gamma ray rejection efficiency of the subtraction method

The major disadvantage of the subtraction method to remove the gamma ray background noise is the need to scale the signals before subtraction to account for solid angle and shielding geometry differences between the two detectors. To ensure the practical use of the probe in theatre blocks, the weighting factor should be insensitive to the variations in the background ray source distribution due to the radiotracer uptake by tumor and normal tissues. This insensitivity mainly depends on the gap between the two detectors.

The source geometry implemented in the simulation is assumed to be representative of the activity distribution encountered in brain tumor surgery, which is one of the potential clinical applications of the positron imaging probe. A cylinder of 140 mm diameter and 100 mm height simulates the geometrical brain phantom. The surgical cavity is modelled by a 30 mm diameter hole on the top of the cylinder. A focal area of tumor tissue, simulated by a 6mm diameter and 1mm thick disk, is placed at the bottom of the cavity. The activity concentration ratio between tumorous and healthy tissues was set to 1.7 according to the concentration of ^{18}F-FDG reported in the literature for high grade glioma and normal brain tissues. The probe is simulated by two 0.5 mm thick scintillating plastic sheets separated by a low density intervening medium with thickness ranging from 0 to 5mm in order to model the light guide and/or the PCB board between the two scintillators. The probe was placed in contact with the tumor disk. The density and atomic composition of brain tissues and detection material were set according to the NIST database.

The gamma ray rejection efficiency of the subtracting method was quantified by calculating the error on the true positron counting rate of the tumor measured by the top scintillator after subtraction. This error is calculated as a function of the distance between the two scintillators for three different weighting factors simulating the variations in the background ray source distribution. These weighting factors were estimated from the ratio between the gamma images measured by the top and the bottom detectors without the tumor disk for 3 different depths of the surgical cavity (10mm, 50mm and 90mm).

2.2.2 Imaging performances

The geometry and physical nature of the two imaging probe architectures are fully modelled (fig.1). For the first configuration, only the front detector was simulated: a plastic scintillator is optically coupled to a 4x4-channel SiPM array composed of 3x3 mm^2 elements (3.2 mm pitch) by means of a PMMA light guide. The second configuration implements two plastic scintillators separated by a light guide. All surfaces are optically polished except the sides of the continuous scintillators and the light guides that were assumed to be ground and coated with a black absorbing paint. The pixelated scintillator was made of 3x3mm² elements separated by a gap of 200µm filled with $BaSO_4$ white diffusing paint (Labsphere 6080). The rear scintillator is optically coupled to the SiPM array. For all configurations, the upper surface of the top scintillator is covered with a 50µm layer of white diffusing paint. A grease layer of 50 µm (BC-630, Bicron) is placed between the scintillator, the light guide and the 300µm thick epoxy coating of the SiPM array. We used the UNIFIED model of the GATE optical photon tracking to describe the photons interactions at the surfaces between two materials. The diffusing paint was assumed to act as a Lambertian reflector. Other optical properties, including the scintillation light yield, refractive index and reflectivity were set according to literature.

For each positron or gamma interaction event in the plastic scintillator, the number of optical photons collected on each SiPM of the array is recorded. The distribution of the number of primary discharges triggered by the photons is calculated from a Poisson-distributed random variable with a mean equal to the total number of photons multiplied by the photon detection efficiency (PDE). The influence of crosstalk and afterpulsing on the measured distribution of the number of photoelectrons (excess noise factor) is also taken into account by considering an exponential distribution probability of the total output charge produced by a primary Geiger discharge with an expectation value equal to n_f (expressed in term of the equivalent number of single fired cells). The thermal noise is also included by adding a random number of photoelectrons to this distribution according to the dark count rate (DCR) and the integration time. The saturation effect due to the finite number of microcells in the SiPM was showed to be negligible. The SiPM features, including PDE (24.5%), DCR (270kHz) and n_f (1.14), were set according to measurements at 20°C and an overvoltage of 1.16V [7]. The position of the interaction event in x and y directions is calculated from the centroid of the distribution of the total output charge provided by the SiPMs of the array. The depth of interaction decoding is based both on the calculation of the standard deviation of this distribution (σ) and the charge ratio between the hottest pixel and the sum of all surrounding pixels (r_z).

Spatial resolution, distortion and depth of interaction decoding were estimated using a pencil beam of 511keV gamma rays or ^{18}F positrons with normal incidence to the surface of the detector. In the centre region of the field of view (four central SiPMs), the source is scanned with a 1.6 mm pitch between each position. The external region to within 1.5 mm of the detector edge was investigated more accurately by using a 0.8mm pitch. Due to the symmetry of the detector, only one eighth of the field of view was investigated. Spatial resolution (FWHM) and bias are calculated from a Gaussian fit to the peak positions. The spatial resolution is corrected of the local bias. For the second background subtraction scheme, two characteristics peak are identified from the light distribution spectrum calculated from the value of σ and r_z, whereby events occurring in the top or the bottom scintillator can be discriminated (fig. 3). The efficiency of the scintillator identification was quantified by calculating the proportion of ill-positioned events for an optimal threshold level between the two peaks of the light distribution spectrum. When the continuous scintillator of the bottom layer is replaced by a pixelated array, a field-flood illumination is also simulated using a 511keV γ source to quantify the identification of the pixel elements. To improve clarity of the paper, only results obtained with 511keV γ ray will be reported. Performances achieved with positrons were shown to be slightly better, due to the higher mean energy deposited in the scintillator.

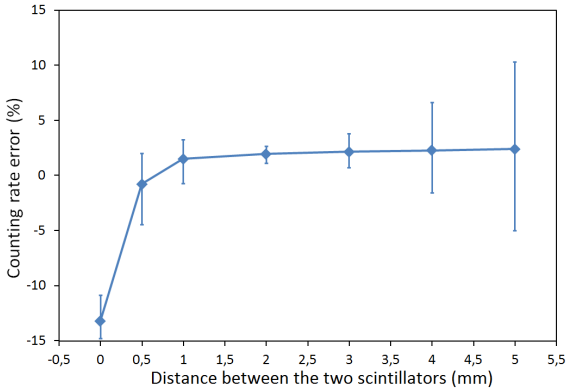

Fig.2. Simulated error on the true positron counting rate of a 6 mm diameter ^{18}F source obtained after subtraction of the gamma contamination as a function of the distance between the two plastic scintillators.

3. Results

3.1 Gamma ray rejection efficiency

Fig. 2 shows the error on the true positron counting rate of the tumor after applying the subtraction method as a function of the distance between the front and the rear detectors. Rejection efficiency close to 98% can be achieved when the gap is between 0.5 and 5 mm. For smaller gaps, error drops because some positrons can interact in both scintillators, leading to an overvaluation of the background gamma noise. The mean error for a gap larger than 1 mm is always greater than 0 due to the gamma contamination coming from the tumor which affects in a different way both scintillators and which are not taken into account by the weighting factor. The error bars in fig.2 represent the variation of the counting rate error when the weighting factor used for the subtraction method is measured in a background γ ray distribution that is not similar to that encountered during the tumor survey. The maximum variation of the positron counting rate was less than 4% for gap ranging from 1 to 4 mm. This shows that the subtraction method is nearly insensitive to the variation in the background γ ray distribution.

3.2 Scintillator identification

The identification error of events occurring in the top or the bottom scintillator obtained from the σ and r_z spectra of the light distribution decreases with the light guide thickness (fig. 3). The discrimination method based on r_z shows better performances whatever the geometry of the rear scintillator. The difference between r_z and σ is due to the non-gaussian distribution of the scintillation light over the array. The advantage of r_z over σ is strongly emphasis with the pixelated detector. For a light guide thickness ranging from 0.5 to 4 mm, the mean identification error in the central region achieved with σ decreases from 33% to 5%, while r_z drops from 8% to only 1%. For both configurations, and both discrimination parameter, the truncation of the light distribution on the edges, which increases with the light guide thickness, strongly degrades the scintillator identification compared to the centre region. The bottom pixelated scintillator narrows this truncation leading to a much more uniform discrimination (absolute variation over the whole surface less than 0.5% for light guides thicker than 2mm).

3.3 Spatial resolution and bias

Fig.4 summarizes the X/Y positioning performances for all imaging probe configurations. As expected, X/Y resolutions achieved with the first configuration degrade when the light guide thickness increases because of the spread of the light distribution.

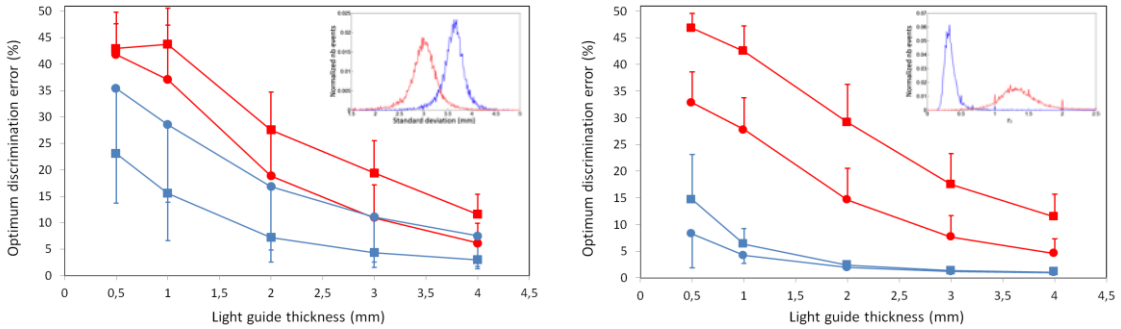

Fig.3 Scintillator identification error as a function of the light guide thickness for a continuous (left) and a pixelated rear scintillator (right). Discrimination is based on the estimation of the σ (red) and r_z (blue) of the light distribution (inset). Mean identification error are reported for testing positions in the center (●) and the edge region (■) of the detection field of view. The error bars (standard deviation) represent the error uniformity over each region. σ (left) and r_z (right) distributions in medallion are for a 2mm thick light guide with a pixilated bottom scintillator. Top and bottom scintillators are presented with blue or red lines, respectively.

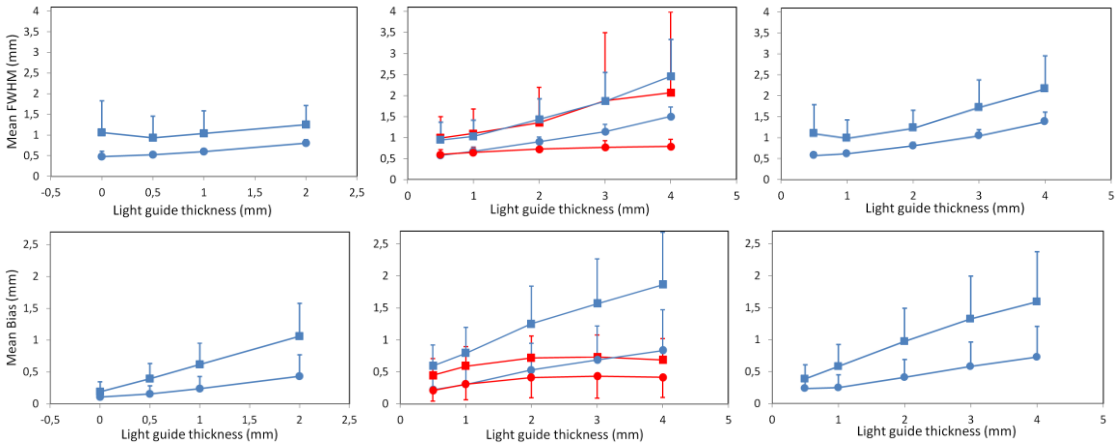

Fig.4. Average resolution (FWHM) and bias over all testing positions as a function of thickness of the light guide for the first (left) and second detector configuration (middle and right, for the continuous and pixelated rear scintillator, respectively). Average resolution and bias are reported for testing positions in the centre (●) and edge regions (■) of the detection field of view. The error bar (standard deviation) represents the resolution and bias uniformity over each region. Top and bottom scintillators are presented with blue or red dots, respectively.

The truncation of the light distribution by the absorbing edges of the detector also increases the FWHM of the peak positions and their bias towards the centre of the detector. For the first configuration, the average spatial resolution over the whole field of view for a 1 mm light guide thickness is 0.8mm FWHM and the mean bias is 0.4mm (fig.5-A). For the second configuration with continuous layers, the spatial resolution and bias achieved with the top scintillator exhibit a behavior similar to the first configuration for equivalent thickness of the optical medium between the scintillator and the SiPM array. Bottom scintillator resolution degrades significantly slower because the thickness of the light guide affects only the part of light that is emitted in the direction of the top scintillator and is reflected back by the diffusing paint. As expected, the spatial resolution of the top scintillator is slightly better when the continuous bottom scintillator is replaced by a pixelated array. Flood field images also show that all pixel elements of the bottom scintillator are clearly resolved with a maximum error on the positioning of interaction of 6% whatever the thickness of the light guide.

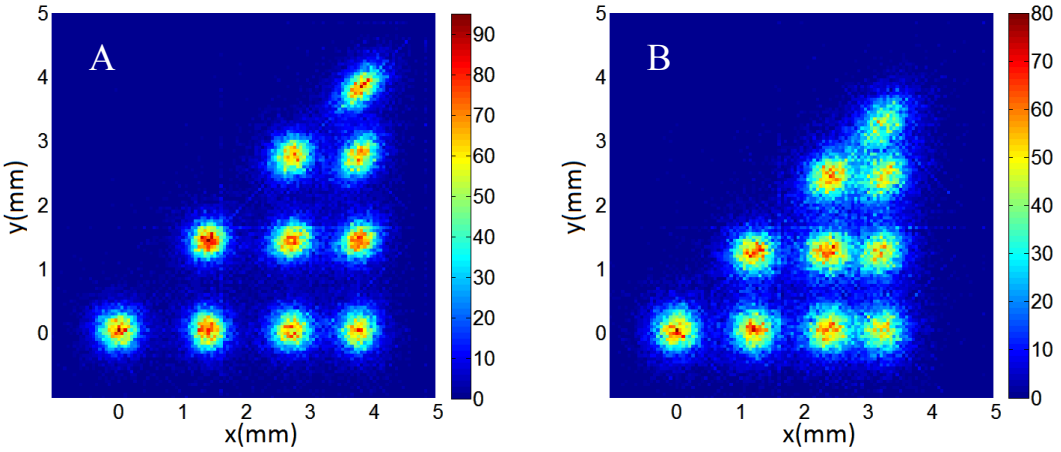

Fig.5. Simulated images of 1.6 mm spaced pencil beams of 511 keV γ rays obtained with the first (1mm thick light guide) (A) and the second configuration (2mm thick light guide and pixilated bottom scintillator) of the positron probe (B).

4.Discussion and conclusion

A simulation study was conducted to optimize the design of a SiPM-based positron imaging probe with gamma ray background rejection capabilities. Different designs were simulated. We first showed that a two layer detection head can perform very good rejection of the background gamma noise with a weak sensitivity to its distribution when the gap between the two detectors is smaller than 4 mm. This close proximity can be achieved with the first configuration based on the stack of two SiPM detectors arrays due to the extreme compactness of the array. This configuration offers submillimetric resolution and bias over the whole field of view for light guide thickness ranging between 0.5 and 1 mm. (fig. 4). These simulation results were validated with preliminary experimental measurements.

The second configuration of the positron imaging probe allows to further reduce the size and the cost of the probe by implementing a single SIPM array. When using a 2 mm thick light guide and a pixelated bottom scintillator, the identification error of events occurring in the top or the bottom scintillator is very low and the spatial performance is only slightly degraded compared to the first configuration with 1 mm thick light guide (average resolution of 1mm FWHM and a mean bias of 0.7 mm over the whole surface) (fig. 5-B). However, further optimizations are still necessary and are currently under testing to improve the trade-off between the accuracy on the layer identification and the spatial performances. This includes the use of bottom scintillator with higher density and light yield (LYSO) to improve both the accuracy of the gamma noise estimation and the identification error between the two scintillators. New optical coatings (specular reflector) and position algorithms (nonlinear least-square modeling of the scintillation light distribution) are also investigated.

References

[1] Barranger E et al., Ann Surg Oncol, vol. 15(1), 15, 2008.
[2] Pitre S et al., Eur J Nucl Med, vol. 30, 339-343, 2003.
[3] Bogalhas F et al., Phys Med Biol, vol. 54, 4439-4453, 2009.
[4] Garcia-Parra R et al., Ann. Nucl. Med., (2011) doi:10.1007/s12149-011-0492-0.
[5] Bonzom S. et al. IEEE Trans. Nucl. Sci., vol. 54 30–41, 2007.
[6] Bogalhas F. et al. Phys. Med. Biol. vol., 54 4439–4453, 2009
[7] Hudin N. et al. Nucl. Instrum. Methods Phys. Res. A 695 (2012) 242-246